haematologica
Journal of the Ferrata Storti Foundation

Interleukin-17–associated inflammation in non-responders and B-cell remodelling after daratumumab in refractory immune thrombocytopenia

by Elsa Drivet, Galina Tsykunova, Ingrid M Egner, Katrine Persgård Lund, Guro Løvik Goll, Hoa Thi Thyuet Tran, Pål Andre Holme, Tor Henrik Anderson Tvedt, Waleed Ghanima, Ludvig A. Munthe and Hassen Kared

Received: April 9, 2026.
Accepted: August 19, 2026.

Citation: Elsa Drivet, Galina Tsykunova, Ingrid M Egner, Katrine Persgård Lund, Guro Løvik Goll, Hoa Thi Thyuet Tran, Pål Andre Holme, Tor Henrik Anderson Tvedt, Waleed Ghanima, Ludvig A. Munthe and Hassen Kared. Interleukin-17–associated inflammation in non-responders and B-cell remodelling after daratumumab in refractory immune thrombocytopenia.
Haematologica. 2026 Sept 3. doi: 10.3324/haematol.2026.301032 [Epub ahead of print]

Interleukin-17-associated inflammation in non-responders and B-cell remodeling after daratumumab in refractory immune thrombocytopenia

Elsa Drivet[1,2], Galina Tsykunova[2,3,4], Ingrid M Egner[1,2], Katrine Persgård Lund[1,2], Guro Løvik Goll[5], Hoa Thi Thyuet Tran[6], Pål Andre Holme[2,7], Tor Henrik Anderson Tvedt[7], Waleed Ghanima[2,3], Ludvig A. Munthe[1,2 §¤], Hassen Kared[1,2 § ¤]

1. Precision Immunotherapy Alliance (PRIMA) and KG Jebsen Centre for B cell Malignancy, Department of Immunology, University of Oslo and Oslo University Hospital, Norway.

2. Institute of Clinical Medicine, University of Oslo, Oslo, Norway

3. Hematology-Oncology, Østfold Hospital Trust, Kalnes, Norway

4. Division of Medicine, Department of Hematology, Haukeland University Hospital, Bergen, Norway

5. Division of Rheumatology and Research, Diakonhjemmet Hospital, Oslo, Norway

6. Department of Hematology, Akershus University Hospital, Oslo, Norway

7. Department of Hematology, Oslo University Hospital, Oslo, Norway

§Corresponding authors: Ludvig A Munthe, l.a.munthe@medisin.uio.no,

Hassen Kared, hassen.kared@medisin.uio.no

¤Co-senior authors

Acknowledgments: The authors thank all clinicians, nurses and patients for providing samples used in this study, as well as the clinic for laboratory medicine (KLM OUS) for the analysis of plasma/serum samples.

This clinical trial was supported by grants from Regional Health Authority South-East, Østfold Hospital Trust, Oslo University Hospital (Norway), the Research Council of Norway (grant number 312780), the Stiftelsen KG Jebsen grant 19. Daratumumab was provided by Janssen Pharmaceutica NV (Beerse, Belgium).

Authorship: Contribution: ED, and HK wrote the first draft of the article. GT, WG, and LAM conceived and designed the trial with the input from all the coauthors. IE and KL organized the biobanking. IE and HK planned and performed O-Link analysis. ED collected clinical daily analyses from all patients. GT, GLG, HTT, PAH, TAT, and WG included study participants. ED, and HK performed statistical analyses. PAH, WG, LAM and HK obtained funding for the study. ED and HK planned and performed flow cytometry analyses. All authors edited the manuscript for important intellectual content. All authors gave final approval of the version to be published and had final responsibility for the decision to submit for publication. This study is registered with ClinicalTrials.gov (NCT04703621) and the European Clinical Trial Register (EudraCT number, 2019-004683-22).

Conflict-of-interest disclosure: G.T. received lecture honoraria from and was part of the advisory board for Janssen, Sanofi, Sobi, and Grifols. H.T.T.T. received consultancy fees from and participated in advisory boards for AbbVie, Grifols, Novartis, and AstraZeneca. P.A.H. received research funding from Bayer, Biogen, Commonwealth Serum Laboratories (CSL), and Sobi; and speaker honorarium from Bayer, BioMarin, CSL, Novo Nordisk, Octapharma, Pfizer, Roche, Takeda, and Sobi. T.H.A.T. received lecture honoraria and fees for participation in advisory boards from Sanofi, Takeda, and Janssen. W.G. received fees for participation in advisory boards from Amgen, Novartis, Pfizer, Principia Biopharma Inc (a Sanofi Company), Sanofi, Sobi, Grifols, UCB, Argenx, Cellphire, Alpine, Kedrion, HiBio, Hutchmed, and Takeda; lecture honoraria from Amgen, Novartis, Pfizer, BMS, Sobi, Grifols, Sanofi, and Bayer; and research grants from Bayer, BMS/Pfizer, UCB, Sobi, and Sanofi. L.A.M. received grants from South East Regional Authority, Research Council of Norway, and Stiftelsen KG Jebsen. The remaining authors declare no competing financial interests.

Data sharing requests should be sent to Hassen Kared (hassen.kared@medisin.uio.no) or Ludvig Munthe (l.a.munthe@medisin.uio.no).

Immune thrombocytopenia (ITP) is an autoimmune disorder characterized by immune-mediated platelet destruction and impaired platelet production (1). Although corticosteroids, thrombopoietin receptor agonists, and anti-CD20 therapies are effective in many patients, a substantial proportion develop refractory disease (2, 3). Long-lived plasma cells, which lack CD20 expression, are thought to sustain autoantibody production and represent a therapeutic target (4, 5).

CD38-targeting monoclonal antibodies such as daratumumab have recently been explored in this setting (6, 7). Clinical studies indicate that daratumumab can induce platelet responses in refractory ITP, although these are not consistently sustained (8-10). The mechanisms underlying this heterogeneity remain incompletely understood.

We performed a longitudinal immunological analysis of 16 patients with chronic refractory ITP enrolled in the DART phase II trial evaluating the anti-CD38 monoclonal antibody daratumumab in pretreated patients with relapsed or refractory disease. The trial was conducted according to the International Council on Harmonization Guidelines for Good Clinical Practice and the Declaration of Helsinki. The ethics committee of each participating institution approved the trial protocol. All patients provided written informed consent before trial entry. Peripheral blood and bone marrow samples were analyzed using spectral flow cytometry and cytokine profiling. Patients were classified according to platelet response at week 24.

Most patients showed an early increase in platelet counts following treatment initiation. However, sustained responses were observed in only a subset of patients, consistent with recent clinical reports (9, 10). Non-responders were generally older and more frequently had undergone splenectomy.

Longitudinal cytokine profiling revealed distinct inflammatory patterns during therapy (Figure 1A, Supplementary Figure S1A). Platelet counts during treatment were inversely associated with IL-6 and IL-18 and positively associated with chemokines (Figure 1B, Supplementary Figure S1B). These relationships were not observed at baseline, suggesting that immune changes during therapy may be more informative than baseline measurements alone. While responders showed a partial reduction in inflammatory mediators over time, non-responders maintained elevated levels of several cytokines, including IL-6, IL-18, and members of the IL-17 family (Figure 1C, Supplementary Figure S1C). Among these, IL-17F and IL-17C remained more consistently elevated in non-responders, suggesting persistent pathogenic IL-17 pathway activation despite CD38-targeted therapy. These findings provide an immunological context for the heterogeneous clinical responses recently observed with CD38-targeted therapy in ITP.

We next examined T-cell associated immune profiles, including proliferation and cytokine secretion (Figure 2A, Supplementary Figure S2A). All ITP patients demonstrated increased secretion of IL-17F compared with healthy donors following TCR stimulation, with elevated IL-17A most pronounced in patients with low platelet counts, whereas patients with higher platelet counts produced higher levels of IL-2 and TNF (Figure 2B). This suggests a preserved T cell fitness in responders and a pathogenic/pro-inflammatory profile in non-responders. Flow cytometric analyses further demonstrated increased frequencies of Th17 cells in all ITP patients and Th1/Th17 hybrid populations in patients with lower platelet counts (Figure 2C, Supplementary Figure S2B). Although IL-17A has been more extensively studied in autoimmunity, persistent elevation of IL-17F may also reflect chronic pathogenic Th17 activation and contribute to sustained inflammatory signaling despite CD38-targeted therapy (11, 12). These observations were accompanied by reduced proliferative T-cell capacity and features of terminal differentiation in $CD8^+$ T cells (CD57, GPR56, SLAMF7) consistent with ongoing immune activation in non-responders (Supplementary Figure S2C-D). Clonal expansion of effector memory/ terminal effector $CD8^+$ T cells has also been described in ITP and may contribute to platelet destruction (13).

We next assessed immune remodeling following CD38 targeting (Figure 3A, Supplementary Figure S3A). Daratumumab induced a marked reduction in CD38 expression across multiple immune compartments, providing pharmacodynamic evidence of effective CD38 targeting (Figure 3B, Supplementary Figure S3B). High-dimensional analysis of the B-cell compartment showed marked remodeling after therapy, with depletion of the $CD38^{high}$ $CD20^{lo}$ plasmablast compartment and relative expansion of naïve and memory populations (Figure 3C, Supplementary Figure S3C). In particular, a $CD38^{high}$ $CD20^{lo}$ plasmablast cluster (cluster 23), which additionally expressed IgD, was prominent in the bone marrow at baseline and was profoundly depleted after therapy in both responders and non-responders, consistent with effective targeting of the $CD38^{high}$ antibody-secreting compartment. The remaining B-cell clusters corresponded predominantly to naïve mature and memory populations by consensus marker classification (14, 15). These observations indicate that depletion of the $CD38^{high}$ plasmablast compartment occurred irrespective of clinical response, suggesting that non-response is not explained by a failure to remodel this compartment. This points instead to a depletion-resistant source of autoantibody production. A $CD38^{low}$, long-lived plasma-cell reservoir, which downregulates CD38 and resides in protected marrow niches, is a well-established, therapy-resistant contributor in antibody-mediated autoimmunity: in refractory systemic lupus erythematosus and lupus nephritis, daratumumab depletes long-lived plasma cells and induces clinical responses, yet a subset of patients still fail to respond, mirroring our findings in ITP (16, 17). Our observations are further consistent with the recent single-cell bone-marrow atlas of ITP, in which a defect in central B-cell tolerance generates autoreactive naïve B cells; such a persistent upstream defect, together with a depletion-resistant plasma-cell reservoir, offers a coherent explanation for the high relapse rates of B-cell-directed therapies even when the plasmablast compartment is effectively cleared (18). As our spectral flow panel did not include intracellular immunoglobulin and had limited resolution of terminally differentiated $CD138^{+}$ plasma cells, direct confirmation of this reservoir in ITP will require dedicated plasma-cell markers and single-cell approaches.

Our findings are consistent with recent clinical studies of CD38-targeted therapy in ITP, including the CM313 study, which demonstrated 89% and 64% platelet response rates at 12 and 24 weeks with a novel anti-CD38 antibody (8). CM313 also reported effective $CD38^{+}$ cell depletion, reduction in IgG levels, and NK cell depletion, immunological effects similarly observed in our cohort (Figure 3B and data not shown). However, direct comparison of response rates is limited by important differences in cohort characteristics: CM313 enrolled a younger population with shorter disease duration, limited prior rituximab exposure, and approximately 65% of patients had detectable platelet glycoprotein autoantibodies at baseline, a profile enriched for antibody-mediated disease. In contrast, our cohort was more heavily pretreated and enriched for refractory, likely T-cell-predominant disease, as reflected by the lower rate of serological autoantibody detection and the predominance of IL-17-associated immune signatures. Notably, CM313 demonstrated efficacy in splenectomised patients, a group refractory to daratumumab in our cohort, further highlighting the impact of patient selection on response. Our longitudinal immune profiling extends beyond clinical outcomes by identifying persistent IL-17-associated inflammation as potential immune correlate of therapeutic resistance, a feature not systematically evaluated in CM313. Whether IL-17 pathway co-targeting could improve outcomes in patients with Th17-predominant ITP warrants prospective investigation.

This study has several limitations. Platelet autoantibodies, measured by MAIPA, were not associated with clinical or immunological responses in our cohort (10), although technical limitations and assay sensitivity may have influenced these analyses. The cohort size is modest and reflects the exploratory nature of the analysis. Prior therapies, age differences, splenectomy status and broader clinical heterogeneity may have influenced immune profiles and treatment responses.

The limited cohort size also reduces statistical power for subgroup analyses and limits definitive conclusions regarding predictive biomarkers. Functional validation of specific pathways was beyond the scope of this study. Nevertheless, the consistency of findings across cytokine and cellular analyses supports the robustness of the observations.

In summary, persistent IL-17-associated inflammation was associated with reduced response to CD38-targeted therapy in refractory ITP. These findings may help identify patients less likely to benefit from this approach and support future investigation of combination strategies targeting inflammatory pathways.

References

1. Cines DB, Blanchette VS. Immune thrombocytopenic purpura. N Engl J Med. 2002;346(13):995-1008.

2. Neunert C, Terrell DR, Arnold DM, et al. American Society of Hematology 2019 guidelines for immune thrombocytopenia. Blood Adv. 2019;3(23):3829-3866.

3. Rodeghiero F, Stasi R, Gernsheimer T, et al. Standardization of terminology, definitions and outcome criteria in immune thrombocytopenic purpura of adults and children: report from an international working group. Blood. 2009;113(11):2386-2393.

4. Audia S, Bonnotte B. Emerging therapies in immune thrombocytopenia. J Clin Med. 2021;10(5):1004.

5. Mahevas M, Michel M, Weill JC, Reynaud CA. Long-lived plasma cells in autoimmunity: lessons from B-cell depleting therapy. Front Immunol. 2013;4:494.

6. Krejcik J, Casneuf T, Nijhof IS, et al. Daratumumab depletes CD38+ immune regulatory cells, promotes T-cell expansion, and skews T-cell repertoire in multiple myeloma. Blood. 2016;128(3):384-394.

7. van de Donk NW, Janmaat ML, Mutis T, et al. Monoclonal antibodies targeting CD38 in hematological malignancies and beyond. Immunol Rev. 2016;270(1):95-112.

8. Chen Y, Xu Y, Li H, et al. A novel Anti-CD38 monoclonal antibody for treating immune thrombocytopenia. N Engl J Med. 2024;390(23):2178-2190.

9. Sun T, Chen Y, Zhang L. Daratumumab in relapsed or refractory pediatric immune thrombocytopenia. N Engl J Med. 2025;392(20):2069-2071.

10. Tsykunova G, Holme PA, Tran HTT, et al. Safety and efficacy of daratumumab in immune thrombocytopenia. Blood Adv. 2026;10(1):143-154.

11. Chang SH, Dong C. IL-17F: regulation, signaling and function in inflammation. Cytokine. 2009;46(1):7-11.

12. Semple JW, Provan D. The immunopathogenesis of immune thrombocytopenia: T cells still take center-stage. Curr Opin Hematol. 2012;19(5):357-362.

13. Malik A, Sayed AA, Han P, et al. The role of CD8+ T-cell clones in immune thrombocytopenia. Blood. 2023;141(20):2417-2429.

14. Carsetti R, Corrente F, Capponi C, et al. Comprehensive phenotyping of human peripheral blood B lymphocytes in pathological conditions. Cytometry A. 2022;101(2):140-149.

15. Carsetti R, Terreri S, Conti MG, et al. Comprehensive phenotyping of human peripheral blood B lymphocytes in healthy conditions. Cytometry A. 2022;101(2):131-139.

16. Ostendorf L, Burns M, Durek P, et al. Targeting CD38 with daratumumab in refractory systemic lupus erythematosus. N Engl J Med. 2020;383(12):1149-1155.

17. Roccatello D, Fenoglio R, Caniggia I, et al. Daratumumab monotherapy for refractory lupus nephritis. Nat Med. 2023;29(8):2041-2047.

18. Sheng Z, Jiang N, Gao Y, et al. A single-cell atlas of bone marrow B cells reveals defective central B-cell tolerance in immune thrombocytopenia. Blood. 2026;147(4):416-430.

Figure legends

Figure 1

Persistent Inflammation distinguishes responders from non-responders to daratumumab

A. Principal component analysis of circulating cytokines. Visualization of cytokines and soluble mediators measured using O-link technology. ITP patients are identified according to platelet counts (low platelet count $<50\times10^9$/L in red; high platelet count $>50\times10^9$/L in blue) and compared with healthy donors (HDs, green). The distribution of patient groups is summarized by automatically generated ellipses. Normalized values of proteins are depicted in Supplementary Figure S1A.

B. Correlation between cytokine levels and platelet counts during therapy. The quantification of cytokines was performed by O-link in the serum of ITP patients at baseline (red dots) or after daratumumab therapy (black dots for weeks 12/16 or 24). The correlations between platelet counts and the concentration of IL-6, or IL-18 were evaluated by Spearman test. Coefficient and two-tailed p-values are indicated on the graphs for the on-therapy samples (black dots). Correlation between chemokine levels and platelet counts is shown in Figure S1B.

C. Cytokine signatures associated with clinical response. Volcano plots show the significant fold change for all cytokines measured in the serum of healthy donors and ITP patients according to the clinical response (responders as R24 or non-responders as NR, pooled time-points). The left panel compares HDs with non-responders (NR); the right panel compares HDs with responders (R24). Only cytokines with $p<0.05$ (* in light red) and $p<0.01$ (** in dark red) are annotated. Concentration of proteins at baseline and week 24 are depicted in the radar plots, Supplementary Figure S1C.

Figure 2

Th17 polarization and T-cell dysfunction characterize resistance

A. High-dimensional analysis of cytokines secreted by stimulated PBMCs. Principal Component Analysis of cytokines measured after anti-CD3/CD28 activation using O-link technology. The ITP patients are segregated according to their platelet counts by a color code (blue/red) and compared to HD (green). The distribution of patient groups is summarized by automatically generated ellipse.

B. Cytokine production by stimulated PBMCs according to platelet response. Cytokines released after TCR stimulation were quantified longitudinally following daratumumab therapy. The comparisons were performed between ITP patients with sustained platelet recovery (blue, $> 50x10^9$/L, pooled time-points at weeks 12/16 and 24), and patients with low platelet counts at baseline or non-responsive to therapy (red) or HDs (green). Mann-Whitney tests were applied with p values represented with *, and ** for $p<0.05$ and $p<0.01$ respectively.

C. Th17 immune deviation in ITP patients. Quantification of Th17 cell frequencies after polyclonal stimulation with PMA/Ionomycin in presence of protein transport inhibitor cocktail. The comparisons were performed between three ITP patients who recovered high platelet counts (blue, $> 50x10^9$/L, n=7 with pooled time-points at weeks 12/16 and 24), and all patients with low platelet counts at baseline (n=14) or non-responsive to therapy at weeks 12/16 (n=14) and 24 (red, n=5) or HDs (green, n=14). Mann-Whitney tests were applied with p values represented with *, and ** for $p<0.05$ and $p<0.01$ respectively. Illustrative dot plots of cytokines secreted by CD4 T cells are represented in Supplementary Figure S2A and frequencies in in Supplementary Figure S2B.

Figure 3

Differential immune remodeling following CD38 targeting

A. High-dimensional analysis of PBMCs during daratumumab therapy. UMAP visualization of immune cell populations analyzed by spectral flow cytometry. Major immune subsets were automatically identified using phenograph clustering according to lineage marker expressions. Clusters were annotated for the main immune cell subsets according to the exclusive expression of CD3 (T cells), CD14 (Monocytes), CD19 (B cells) and CD56 (NK cells), left. Longitudinal distribution of immune cells from ITP patients was visualized by UMAP on density plots (middle-right).

B. Quantification of $CD38^{+}$ immune cells during therapy. Frequencies of CD38- expressing immune cells (B cells, T cells, monocytes, NK cells) were evaluated longitudinally in PBMCs (top row at baseline, 12/16 weeks and 24 weeks) and bone marrow mononuclear cells (BMMCs, lower row at baseline, and 16 weeks). Healthy donor reference values (median from 6 donors) are indicated by dotted lines. Significant Kruskal-Wallis test (PBMCs) or paired t test (BMMCs) p values are represented with **, *** or **** for $p<0.01$, $p<0.001$ and $p<0.0001$ respectively. Gating strategy is described in Supplementary Figure S3A and CD38 expression in cell subsets of two representative patients are described in Supplementary Figure S3B.

C. Bone-marrow B-cell remodelling in responders and non-responders after daratumumab. Equal number of $CD19^{+}$ B cells (2,000 per sample) from bone-marrow aspirates of responders (n=3) and non-responders (n=7) were concatenated and projected into a shared UMAP embedding, with clusters identified by the Phenograph algorithm. Density plots show the distribution of B-cell clusters in bone marrow at baseline (left) and post-therapy (weeks 12/16), together with the density difference (post-therapy minus baseline, right), in which red indicates clusters gained and blue clusters lost after therapy; the three clusters with the largest change are labelled (▲ gained, ▼ lost). Dashed contours delineate B-cell subsets assigned by consensus marker classification following established criteria (plasmablast, $CD24^{-}CD38^{high}$; naïve mature, $CD27^{-}CD21^{+}IgD^{+}$; class-switched memory, $CD27^{+}IgD^{-}IgG^{+}$; unswitched memory, $CD27^{+}IgD^{+}$; atypical memory, $CD21^{-}CD27^{-}$), with representative cluster numbers indicated. Cluster phenotypes and normalized marker expression are detailed in Supplementary Figure S3C.

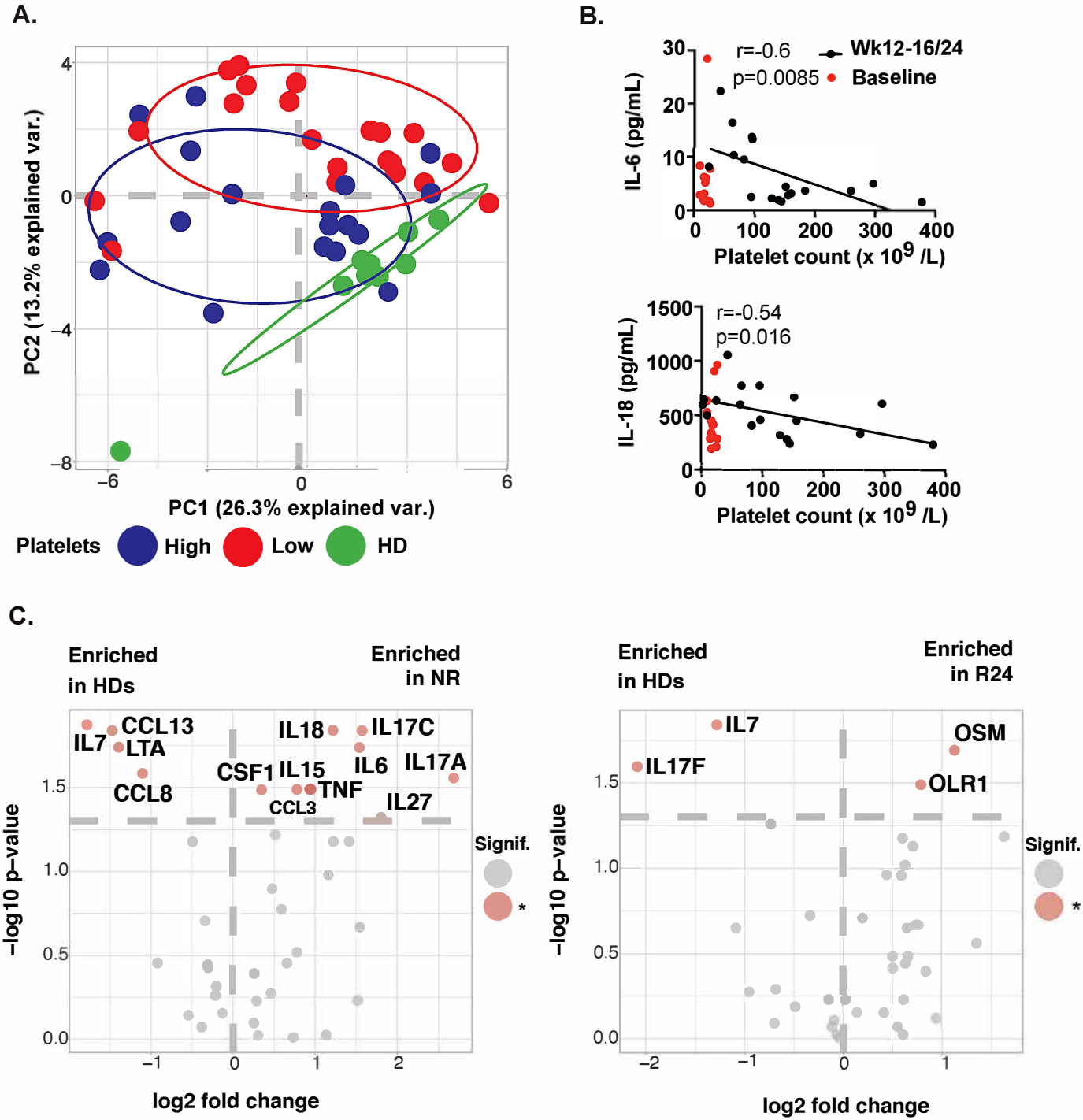
A.
PC2 (13.2% explained var.)
PC1 (26.3% explained var.)
Platelets
High
Low
HD
B.
r=-0.6
p=0.0085
Wk12-16/24
Baseline
IL-6 (pg/mL)
Platelet count (x 10^9 /L)
r=-0.54
p=0.016
IL-18 (pg/mL)
Platelet count (x 10^9 /L)
C.
Enriched in HDs
Enriched in NR
IL7
CCL13
LTA
CCL8
IL18
IL17C
CSF1
IL15
IL6
IL17A
TNF
CCL3
IL27
Signif.
−log10 p−value
log2 fold change
Enriched in HDs
Enriched in R24
IL7
IL17F
OSM
OLR1
Signif.
−log10 p−value
log2 fold change

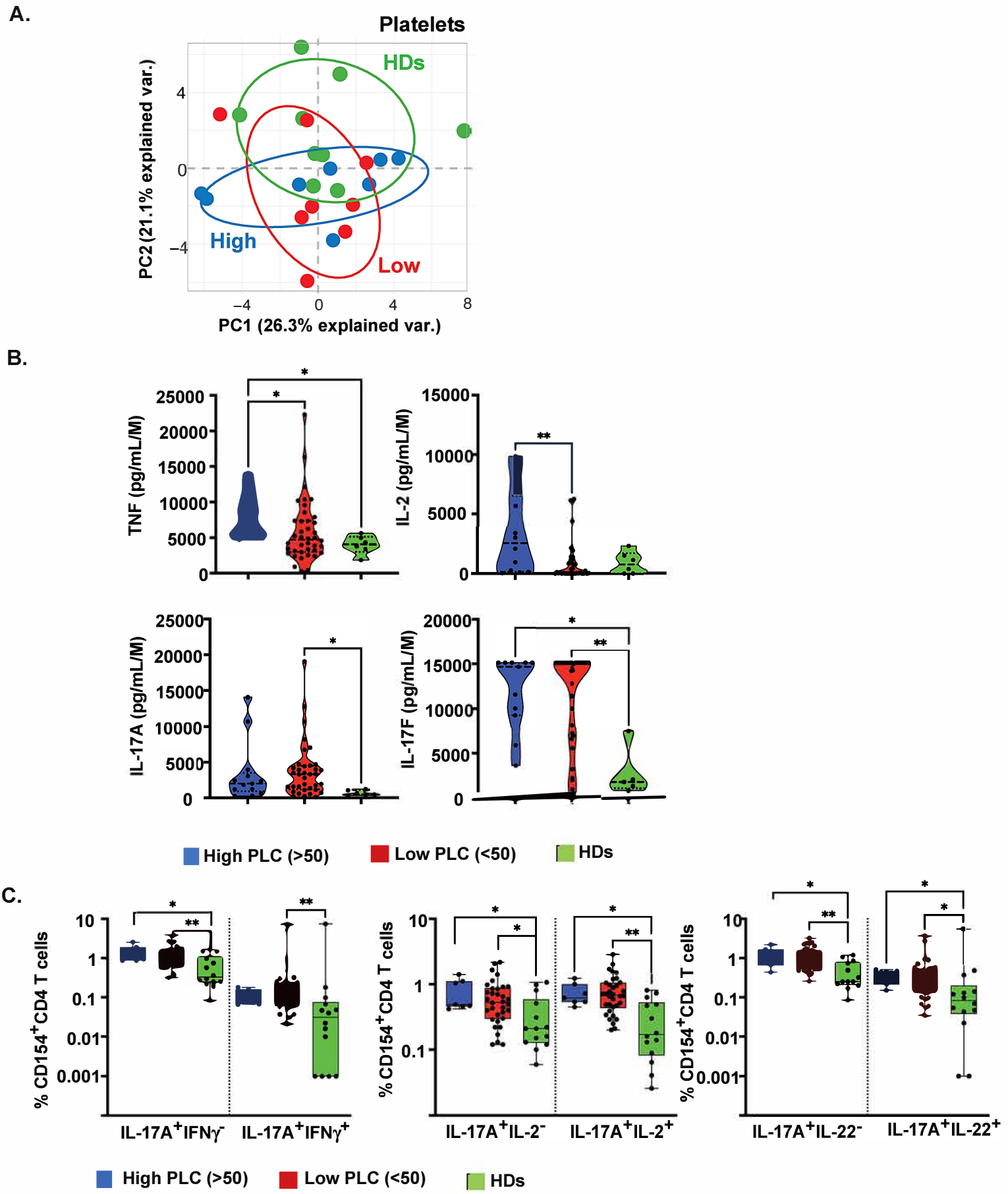
A.
Platelets
HDs
High
Low
PC2 (21.1% explained var.)
PC1 (26.3% explained var.)
B.
TNF (pg/mL/M)
IL-2 (pg/mL/M)
IL-17A (pg/mL/M)
IL-17F (pg/mL/M)
High PLC (>50)
Low PLC (<50)
HDs
C.
% CD154+CD4 T cells
IL-17A+IFNγ-
IL-17A+IFNγ+
IL-17A+IL-2-
IL-17A+IL-2+
IL-17A+IL-22-
IL-17A+IL-22+
High PLC (>50)
Low PLC (<50)
HDs

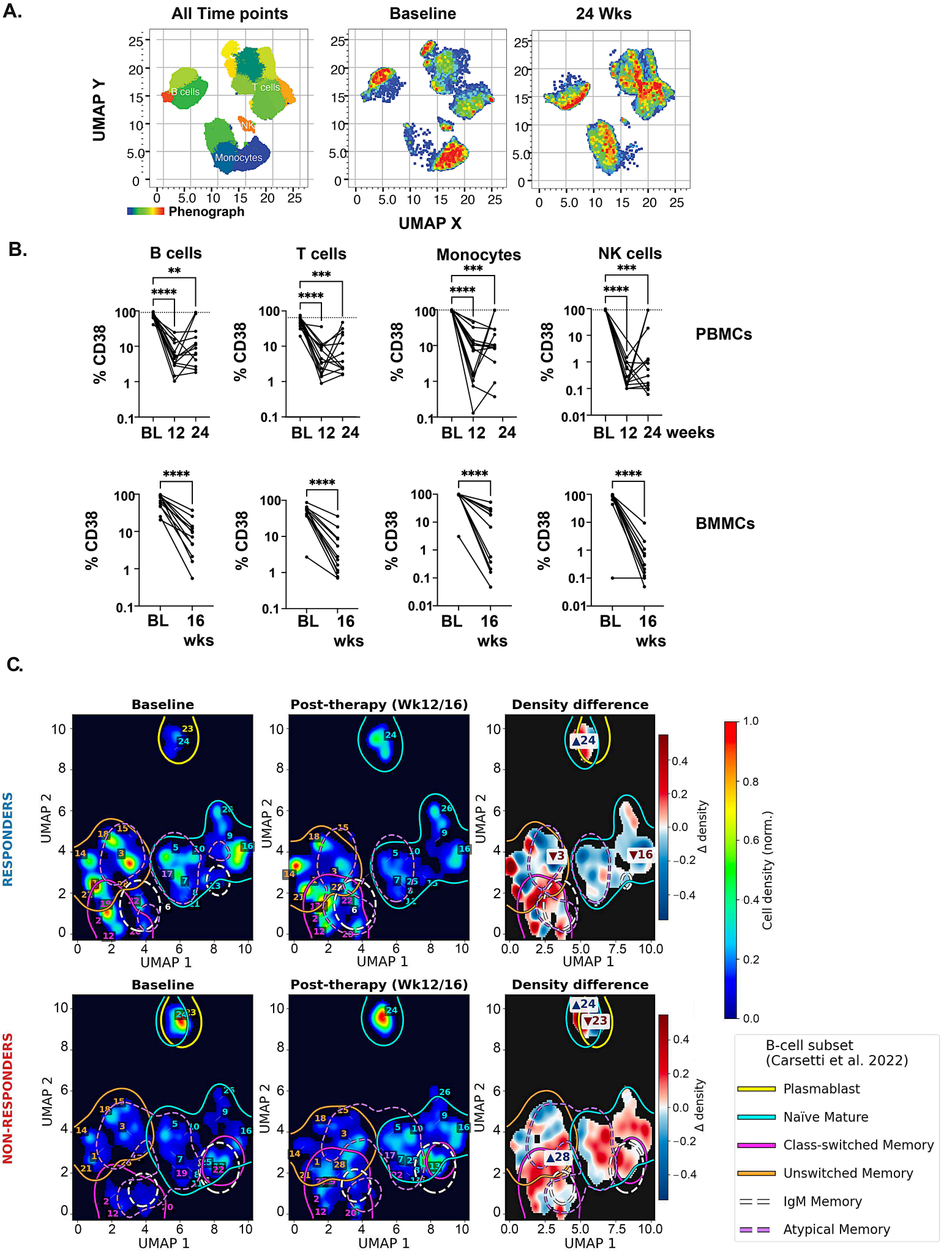
A.
All Time points
Baseline
24 Wks
UMAP Y
UMAP X
B cells
T cells
NK
Monocytes
Phenograph
B.
B cells
T cells
Monocytes
NK cells
% CD38
PBMCs
BMMCs
BL 12 24
BL 12 24 weeks
BL 16 wks
C.
RESPONDERS
NON-RESPONDERS
Baseline
Post-therapy (Wk12/16)
Density difference
UMAP 1
UMAP 2
Δ density
Cell density (norm.)
B-cell subset
(Carsetti et al. 2022)
Plasmablast
Naïve Mature
Class-switched Memory
Unswitched Memory
IgM Memory
Atypical Memory

Supplementary Data and Materials

Inventory

Supplementary Figures

Supplementary Legends

Figure S1

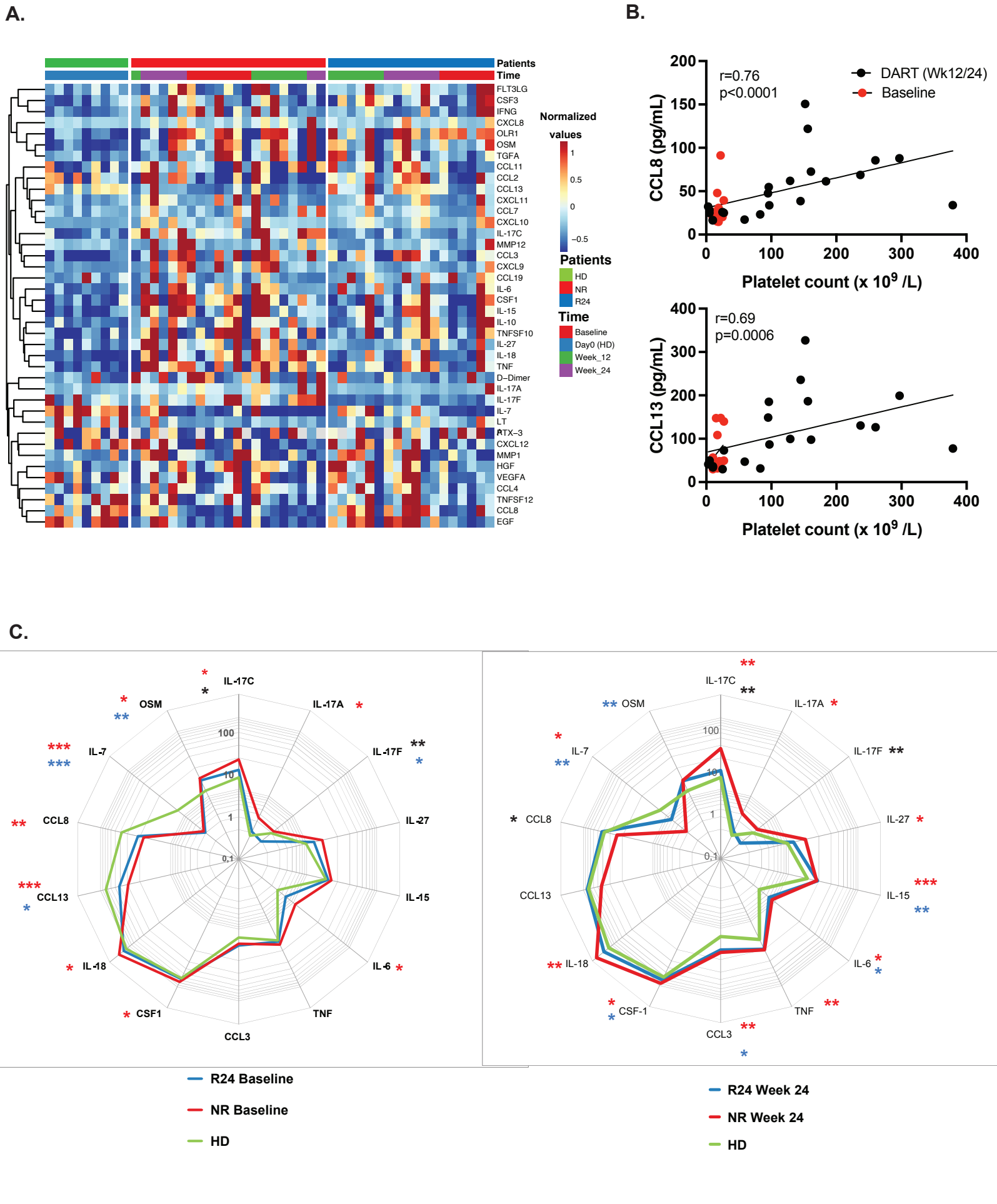
A.
Patients
Time
FLT3LG
CSF3
IFNG
CXCL8
OLR1
OSM
TGFA
CCL11
CCL2
CCL13
CXCL11
CCL7
CXCL10
IL-17C
MMP12
CCL3
CXCL9
CCL19
IL-6
CSF1
IL-15
IL-10
TNFSF10
IL-27
IL-18
TNF
D-Dimer
IL-17A
IL-17F
IL-7
LT
PTX-3
CXCL12
MMP1
HGF
VEGFA
CCL4
TNFSF12
CCL8
EGF
Normalized values
1
0.5
0
−0.5
Patients
HD
NR
R24
Time
Baseline
Day0 (HD)
Week_12
Week_24
B.
r=0.76
p<0.0001
DART (Wk12/24)
Baseline
CCL8 (pg/mL)
Platelet count (x 10^9 /L)
r=0.69
p=0.0006
CCL13 (pg/mL)
Platelet count (x 10^9 /L)
C.
IL-17C
IL-17A
IL-17F
IL-27
IL-15
IL-6
TNF
CCL3
CSF1
IL-18
CCL13
CCL8
IL-7
OSM
R24 Baseline
NR Baseline
HD
R24 Week 24
NR Week 24
HD

Figure S2

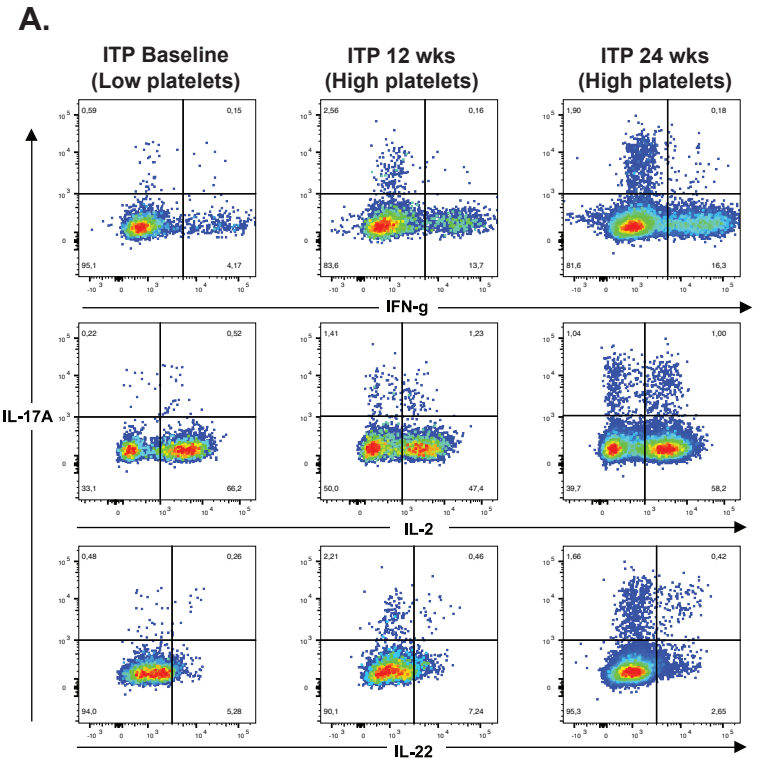
A.
ITP Baseline (Low platelets)
ITP 12 wks (High platelets)
ITP 24 wks (High platelets)
IFN-g
IL-17A
IL-2
IL-22

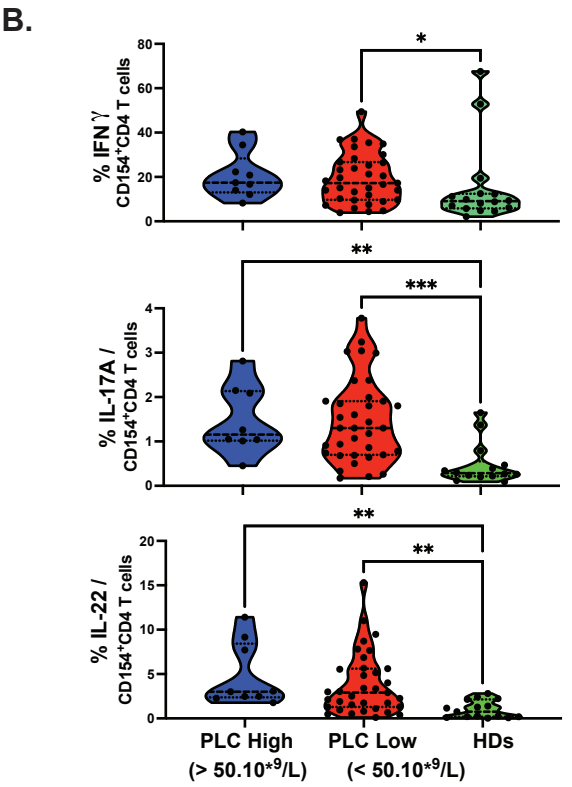
B.
% IFNγ CD154+CD4 T cells
% IL-17A / CD154+CD4 T cells
% IL-22 / CD154+CD4 T cells
PLC High (> 50.10*9/L)
PLC Low (< 50.10*9/L)
HDs

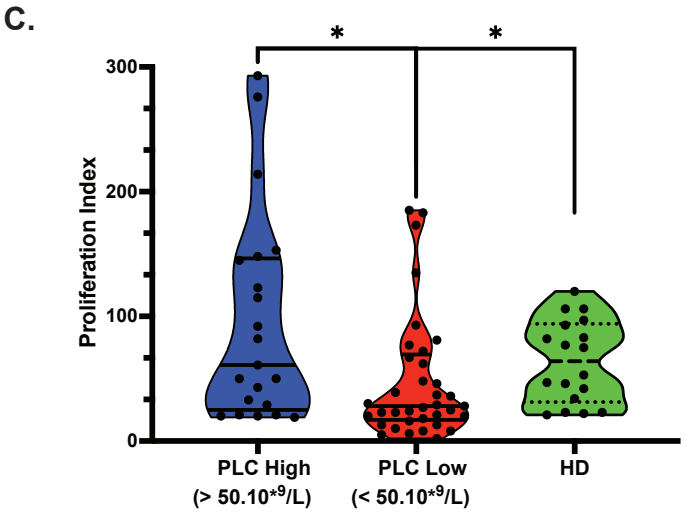
C.
Proliferation Index
PLC High (> 50.10*9/L)
PLC Low (< 50.10*9/L)
HD

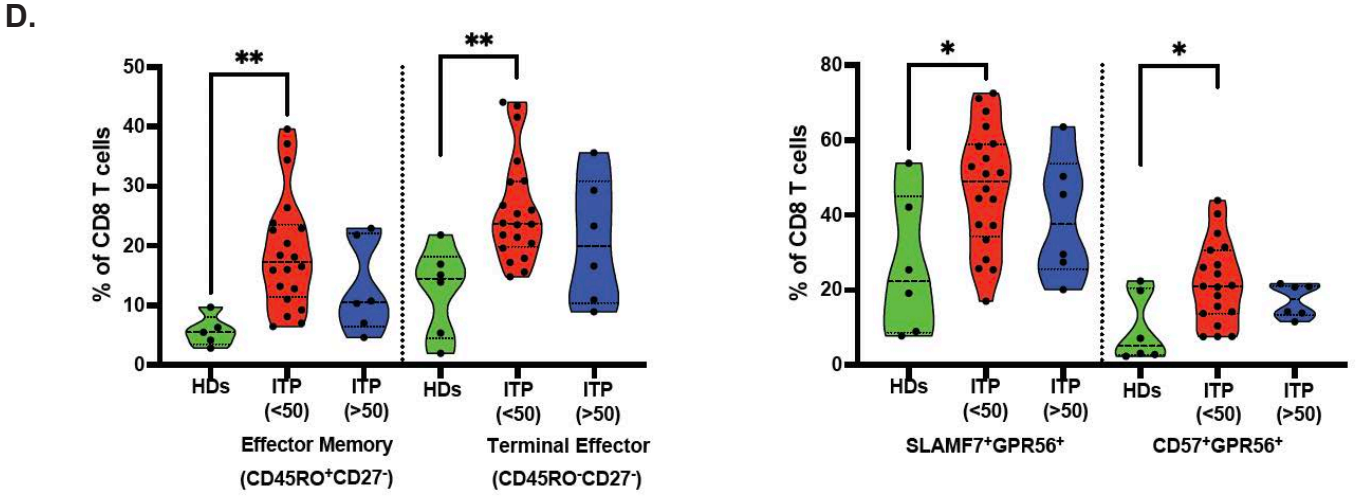
D.
% of CD8 T cells
HDs
ITP (<50)
ITP (>50)
Effector Memory (CD45RO+CD27-)
Terminal Effector (CD45RO-CD27-)
SLAMF7+GPR56+
CD57+GPR56+

Figure S3

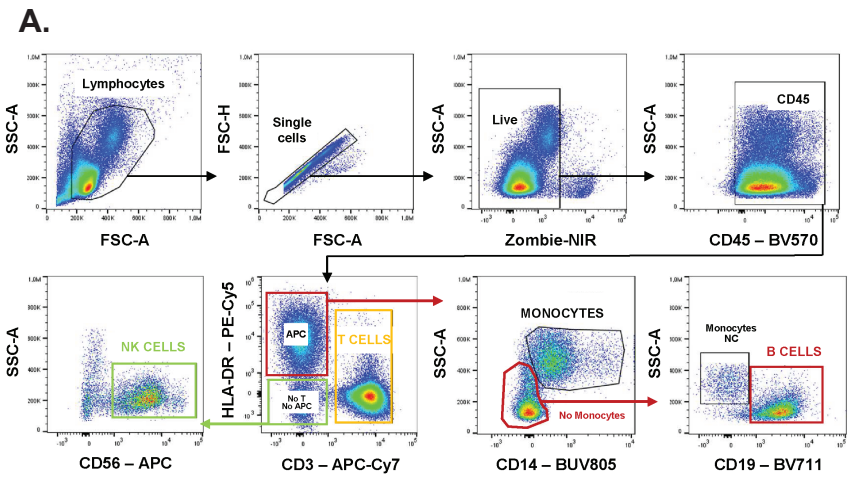
A.
Lymphocytes
SSC-A
FSC-A
Single cells
FSC-H
FSC-A
Live
SSC-A
Zombie-NIR
CD45
SSC-A
CD45 – BV570
NK CELLS
SSC-A
CD56 – APC
APC
T CELLS
No T No APC
HLA-DR – PE-Cy5
CD3 – APC-Cy7
MONOCYTES
SSC-A
No Monocytes
CD14 – BUV805
Monocytes NC
B CELLS
SSC-A
CD19 – BV711

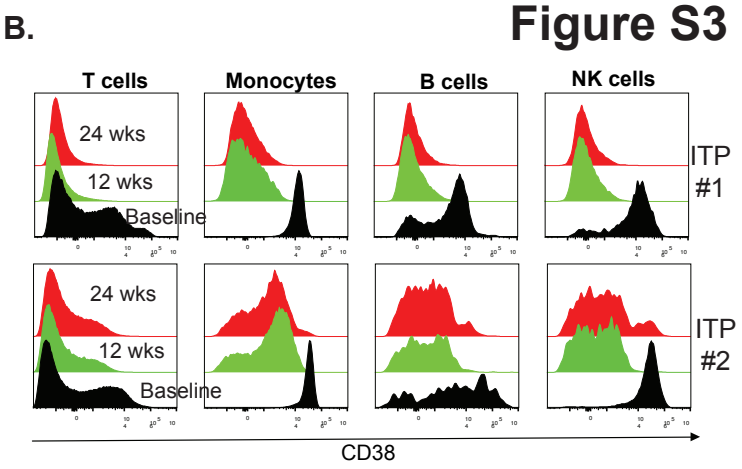
B.
T cells
Monocytes
B cells
NK cells
24 wks
12 wks
Baseline
ITP #1
24 wks
12 wks
Baseline
ITP #2
CD38

C.

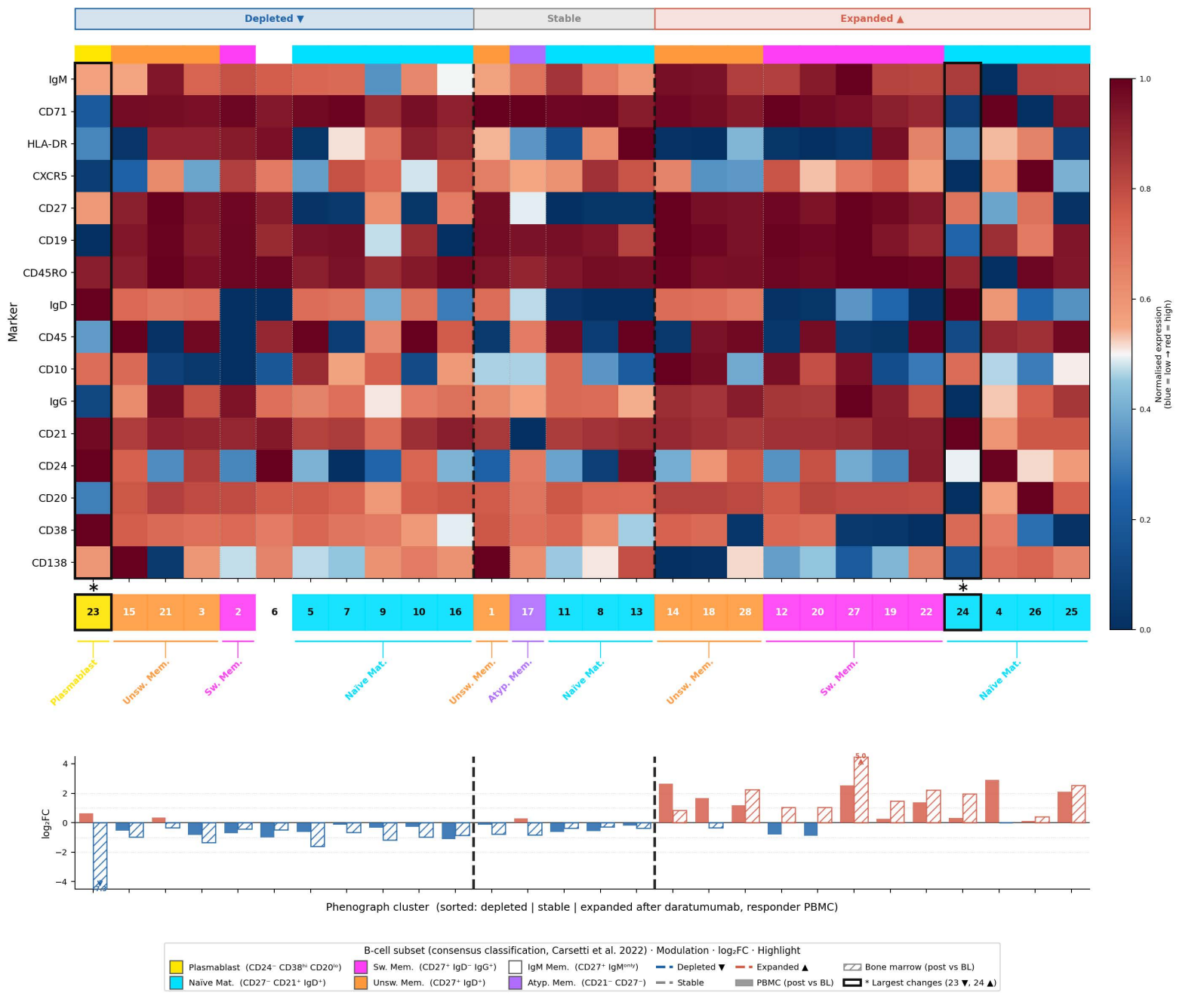
Depleted ▼
Stable
Expanded ▲
IgM
CD71
HLA-DR
CXCR5
CD27
CD19
CD45RO
IgD
CD45
CD10
IgG
CD21
CD24
CD20
CD38
CD138
Marker
Normalised expression (blue = low → red = high)
23 15 21 3 2 6 5 7 9 10 16 1 17 11 8 13 14 18 28 12 20 27 19 22 24 4 26 25
Plasmablast
Unsw. Mem.
Sw. Mem.
Naive Mat.
Unsw. Mem.
Atyp. Mem.
Naive Mat.
Unsw. Mem.
Sw. Mem.
Naive Mat.
log₂FC
Phenograph cluster (sorted: depleted | stable | expanded after daratumumab, responder PBMC)

B-cell subset (consensus classification, Carsetti et al. 2022) · Modulation · log₂FC · Highlight
Plasmablast (CD24⁻ CD38ʰⁱ CD20ˡᵒ)
Naive Mat. (CD27⁻ CD21⁺ IgD⁺)
Sw. Mem. (CD27⁺ IgD⁻ IgG⁺)
Unsw. Mem. (CD27⁺ IgD⁺)
IgM Mem. (CD27⁺ IgMᵒⁿˡʸ)
Atyp. Mem. (CD21⁻ CD27⁻)
Depleted ▼
Stable
Expanded ▲
PBMC (post vs BL)
Bone marrow (post vs BL)
* Largest changes (23 ▼, 24 ▲)

Supplementary Figures

Figure S1

Inflammation and daratumumab in ITP patients

(A) Inflammatory signature of ITP patients and CD38-targeted therapy. Systemic inflammation was characterized longitudinally from the serum of patients with ITP by O-link during DART (n=13) and compared to healthy donors (n=10). A cold-to-hot heatmap represents the relative expression of pro-inflammatory markers, with an automatic hierarchical clustering. The top rows indicate the clinical information of the patients and are detailed on the right side of the heatmap. Healthy donors with normal platelet count in the absence of documented pathology (>100 $\times 10^9$/L) were collected at Day 0.

(B) Correlation between platelet counts and chemokine levels during therapy (weeks 12–24). Each dot represents an individual sample; Spearman correlation coefficients and two-tailed p-values are indicated on the graphs after therapy (black dots).

(C) Dynamic of inflammation in ITP patients treated with CD38-targeted therapy. Quantification of significant cytokines and chemokines at baseline or final end-point according to daratumumab responsiveness (Responders as R24 versus Non-responders as NR). Median concentrations detected in R24 (blue) or NR (red) ITP patients and HDs are represented in pg/mL. Proteins with significant differences as $p<0.05$ (*), $p<0.01$ (**) and $p<0.001$ (***) are annotated with the following color code: blue for HD vs R24, red for HD vs NR and black for NR vs R24.

Figure S2

Functionality of T cells and daratumumab in ITP patients

(A) Th17 -immune deviation patients with ITP treated with anti-CD38 targeted therapy. Representative dot plots of polyclonally stimulated CD4 T cells from responder ITP patients at longitudinal time-points. Samples were stimulated overnight by PMA/Ionomycin, before fixation, permeabilization and intracellular staining. After exclusion of debris, lymphocytes were gated on viable single cells expressing CD4 with upregulated CD154.

(B) Effector profile of CD4 T cells during therapy. Quantification of cytokines-secreting CD4 T cells frequencies after polyclonal stimulation in ITP patients after successful therapy at both time-points (blue, week 12/16 and 24, n=9), in non-responders (red, all time points with low platelet counts, n=36) or HD (green, n=16)**.** Mann-Whitney tests were applied with p values represented with *, and ** for $p<0.05$ and $p<0.01$ respectively.

(C) Proliferative capacity of T cells during therapy. The proliferation of PBMCs was measured after 5 days of stimulation with anti-CD3/CD28 microbeads before the addition and incorporation of tritiated [^{3}H]-thymidine in the proliferating cells. Proliferation of stimulated PBMCs were compared from ITP patients with high (>50 x10^9/L, n=21) with versus low platelet counts (<50 x10^9/L, n=38) and HDs (standard platelet count, n=14), independently of timepoints. Mann-Whitney tests were applied with p values represented with * for $p<0.05$.

(D) Differentiation of CD8 T cell subsets and therapy responsiveness. Phenotype of T cells was performed by flow cytometry. ITP patients were classified according to the platelet count (>50, responsive to daratumumab) at week 12/16 or 24, and compared to patients with low platelet count (<50), either at baseline or after relapses. Mann-Whitney tests were applied with p values represented with *, and ** for $p<0.05$ and $p<0.01$ respectively.

Figure S3

Immune remodeling following CD38-targeted therapy.

(A) Identification of immune cells. Gating strategy used in PBMCs from ITP patients to quantify the main immune cell subsets by spectral flow cytometry. After the exclusion of doublets, dead cells, and debris, live single $CD45^+$cells were further identified as T and non-T cells based on CD3 expression. The non-T cells were divided into antigen-presenting cells (APC) based on HLA-DR expression, including monocytes (CD14) and B cells (CD19). The $CD3^-HLA\text{-}DR^-$ population was used to identify NK cells through the expression of CD56. A similar strategy was used for BMMCs.

(B) CD38 expression and daratumumab. Longitudinal follow-up of CD38 expression shown in overlaid histogram for T-cells, Monocytes, B cells and NK cells in two representative ITP patients (#1 and #2) at baseline, 12/16, and 24 weeks after daratumumab initiation.

(C) Phenotypic characterization of B-cell clusters. The normalized mean expression of each marker per cluster is represented as a blue-to-red heatmap (blue = low, red = high; arcsinh transformation, cofactor 5). Clusters are sorted by modulation after daratumumab therapy (depleted | stable | expanded; separated by thick dashed lines), then by B-cell subset within each group (dotted lines). B-cell subsets were assigned according to consensus phenotypic criteria (Carsetti et al., Cytometry A 2022): Plasmablasts ($CD24^-$ $CD38^{hi}$ $CD20^{lo}$), Naïve Mature ($CD27^-$ $CD21^+$ IgD^+), Class-switched Memory ($CD27^+$ IgD^- IgG^+), Unswitched Memory ($CD27^+$ IgD^+), IgM Memory ($CD27^+$ IgM-only), and Atypical Memory ($CD21^-$ $CD27^-$). Cluster numbers are shown in colour-coded badges at the bottom of the heatmap. Bar charts show the $\log_2$ fold change in cluster frequency after therapy relative to baseline (solid bars: PBMC, post-therapy [Wk16/24 pooled] vs baseline; hatched bars: bone marrow, post-therapy [Wk12/16 pooled] vs baseline; red = expanded, blue = depleted). Clusters 23

and 24, marked with an asterisk and a bold outline, are the two clusters showing the largest changes after therapy: cluster 23, a bone-marrow IgD^{+} $CD38^{hi}$ plasmablast population, is the most strongly depleted, while the adjacent CD38-intermediate cluster 24 (naïve mature) expands as the plasmablast compartment is cleared (see Figure 3C).